

Investigation of proton radioactivity with the effective liquid drop model^{*}

SHENG Zong-Qiang(圣宗强)^{1;1)} SHU Liang-Ping(舒良萍)¹ FAN Guang-Wei(樊广伟)²
MENG Ying(孟影)¹ QIAN Jian-Fa(钱建发)¹

¹ School of Science, Anhui University of Science and Technology, Huainan 232001, China

² School of Chemical Engineering, Anhui University of Science and Technology, Huainan 232001, China

Abstract: Proton radioactivity has been investigated using the effective liquid drop model with varying mass asymmetry shapes and effective inertial coefficients. An effective nuclear radius constant formula replaces the old empirical one in the calculations. The theoretical half-lives are in good agreement with the available experimental data. All the deviations between the calculated logarithmic half-lives and the experimental values are less than 0.8. The root-mean-square (rms) deviation is 0.523. Predictions for the half-lives of proton radioactivity are made for elements across the periodic table. From the theoretical results, there are 11 candidate nuclei for proton radioactivity in the region $Z < 51$. In the region $Z > 83$, no nuclei are suggested as probable candidate nuclei for proton radioactivity within the selected range of half-lives studied.

Key words: proton radioactivity, effective liquid drop model, half-life, exotic decay

PACS: 23.50.+z, 21.10.Tg, 21.60.-n **DOI:** 10.1088/1674-1137/39/2/024102

1 Introduction

Nuclear decays, including alpha, beta and gamma decays, have been studied for more than a century, employing many forms of theory and experiment [1–3]. With the development of radioactive ion beams and related experimental facilities, exotic nuclear physics has become an extremely interesting topic. People can explore the unknown regions of the periodic table and look for many fundamentals in nuclear physics through studies of exotic nuclei [4–10]. The investigation of exotic nuclei has led to the discovery of a new form of radioactivity — proton radioactivity.

Proton radioactivity was observed for the first time in the decay of an isomeric state of ^{53}Co [11, 12]. Since then, a number of proton-emitting nuclei have been found in the region from $Z=51$ to $Z=83$ [13, 14]. These nuclei can emit protons from their ground states or low-lying isomeric states. It is believed that more proton-emitting nuclei will be discovered in the future.

Proton radioactivity can be used as an excellent tool to extract rich nuclear structure information such as shell structure, fine structure, wave function of the parent nucleus, etc. [15–17]. Therefore, it is very important to learn more about proton radioactivity.

Many theoretical approaches and models have been employed to investigate proton radioactivity [18–28]. There have also been many experiments for measuring proton radioactivity [29–39]. In [40, 41], Gonçalves and Duarte proposed the effective liquid drop model to describe exotic decays. Two kinds of shape parametrization modes and two kinds of inertial coefficients are introduced in this model. Strikingly, one can reproduce the data of alpha and exotic decays by using only two parameters — the nuclear radius constant r_0 and the preexponential factor λ_0 . In our previous work, we have investigated cluster radioactivity using this model and achieved excellent results [42].

In this work, we will investigate proton radioactivity by using the effective liquid drop model with varying mass asymmetry shapes and effective inertial coefficients. In view of the importance of r_0 for this model, an effective nuclear radius constant formula will be introduced instead of the empirical one. Systematic calculations of the proton radioactivity will be performed across the periodic table.

This paper is organized as follows. In Section 2, a brief review of the theoretical framework is provided. In Section 3, numerical results and discussions are presented. A summary is given in Section 4.

Received 6 May 2014

^{*} Supported by National Natural Science Foundation of China (11247001), Natural Science Foundation of the Higher Education Institutions of Anhui Province, China (KJ2012A083, KJ2013Z066) and Anhui Provincial Natural Science Foundation (1408085MA05)

1) E-mail: zqsheng@aust.edu.cn

©2015 Chinese Physical Society and the Institute of High Energy Physics of the Chinese Academy of Sciences and the Institute of Modern Physics of the Chinese Academy of Sciences and IOP Publishing Ltd

2 Theoretical framework

In this section, we give a brief theoretical framework. One can find the details of the model in [40, 41]. The decaying system can be regarded as two intersectant spherical fragments with different radii. The shape configuration and geometric parameters are shown in Fig. 1.

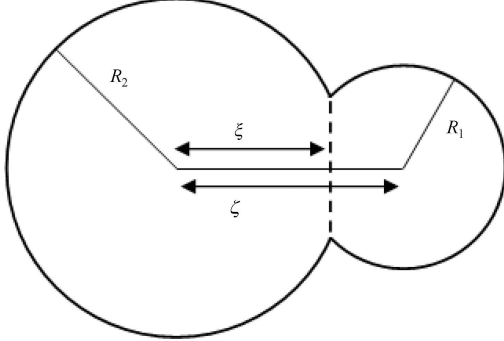


Fig. 1. Shape parametrization of a dinuclear system. The two spherical segments radii are R_1 and R_2 respectively. The distance between the geometrical centers of the two spherical fragments is marked ζ . ξ is the distance from the plane of the intersection to the geometrical center of the heavier fragment.

There are four geometric shape parameters (R_1 , R_2 , ζ , ξ) used to describe the dinuclear system. Three constraint relations used in the model are given in the following three equations. First,

$$2(R_1^3 + R_2^3) + 3[R_1^2(\zeta - \xi) + R_2^2\xi] - [(\zeta - \xi)^3 + \xi^3] - 4R_m^3 = 0, \quad (1)$$

where R_m denotes the radius of the parent nucleus. Secondly,

$$R_1^2 - R_2^2 - (\zeta - \xi)^2 + \xi^2 = 0. \quad (2)$$

Thirdly, at the end of the pre-scission phase, the system will reach a critical state. At this time, the radii of the two spherical fragments are denoted as \bar{R}_1 and \bar{R}_2 for the cluster and the daughter nucleus, respectively. In the mode of varying mass asymmetry, the radius of the light fragment is fixed as

$$R_1 - \bar{R}_1 = 0. \quad (3)$$

In such a picture, the problem can conveniently be reduced to the one-dimensional barrier penetrability problem, and the quantum transition rate can be similarly calculated in accordance with the Gamow alpha decay theory [43]. The expression of the barrier penetrability factor is written as

$$\mathcal{P} = \exp \left\{ -\frac{2}{\hbar} \int_{\zeta_0}^{\zeta_C} \sqrt{2\mu_{\text{eff}}(V-Q)} d\zeta \right\}, \quad (4)$$

where μ_{eff} is the effective inertial coefficient defined in [41]. ζ_0 and ζ_C are respectively the inner and outer turning points. ζ_0 is written as $\zeta_0 = R_m - \bar{R}_1$. In view of the

importance of angular momentum for proton radioactivity, ζ_C is written as

$$\zeta_C = \frac{Z_1 Z_2 e^2}{2Q} + \sqrt{\left(\frac{Z_1 Z_2 e^2}{2Q} \right)^2 + \frac{l(l+1)\hbar^2}{2\mu_{\text{eff}}Q}}. \quad (5)$$

Q is the decay energy and V is the total one-dimensional effective liquid drop potential. The decay energy Q is calculated by the relation $Q = M - M_1 - M_2$, where the masses in the Q value expression are extracted from the latest atomic mass table [44]. For details of the meanings and the expression of V , please see [40].

The final radii of the fragments are written as

$$\bar{R}_i = \left(\frac{Z_i}{Z_m} \right)^{1/3} R_m. \quad (6)$$

Z_m and R_m are the proton number and radius of the parent nucleus. Z_i is the proton number of the fragment.

As mentioned in the introduction, the nuclear radius is of great importance in the present calculation. Previously, a constant r_0 was always employed in the calculation. However, it is well known from available experimental data that the nuclear radius constant r_0 is far from being constant. For this reason, the radius of the parent nucleus is determined by a more precise formula which includes the isospin-dependence:

$$R_m = r_0 A_m^{1/3} = \frac{1.38}{1.20} \times \left(1.2332 + \frac{2.8961}{A_m} - 0.18688 \times I \right) A_m^{1/3}, \quad (7)$$

where I is the relative neutron excess $I = (N_m - Z_m)/A_m$. In the present work, we will use this formula to replace the empirical $R_m = 1.38 A_m^{1/3}$.

The decay rate is calculated by

$$\lambda = \lambda_0 \mathcal{P}, \quad (8)$$

where λ_0 is the preexponential factor. The value of λ_0 is written as [45]:

$$\lambda_0 = 0.5 \times 10^{21} \text{ s}^{-1}. \quad (9)$$

With λ_0 fixed, the half-life can be calculated by

$$T = \ln 2 / \lambda. \quad (10)$$

3 Numerical results and discussion

The calculated half-lives of proton radioactivity are listed in Table 1 and the available experimental data are also included for comparison. We only list the results for the most probable proton decay (ground-state to ground-state transitions). For cluster radioactivity, the angular momentum carried by the cluster is not very large ($l \leq 6$) and the centrifugal barrier is much lower than the Coulomb barrier. The contribution of the angular

Table 1. The theoretical half-lives of proton radioactivity. The experimental Q values are extracted from [44]. All the experimental half-lives and l values are from [14]. Q value is in MeV, and half-life T in seconds.

No.	nucleus	Z	l/\hbar	Q	\mathcal{P}	$\lg T_{\text{Theo.}}$	$\lg T_{\text{Exp.}}$
1	^{105}Sb	51	2	0.483	8.91×10^{-24}	1.830	2.049
2	^{109}I	53	2	0.820	2.35×10^{-17}	-4.592	-3.987
3	^{112}Cs	55	2	0.814	3.72×10^{-18}	-3.791	-3.301
4	^{113}Cs	55	2	0.974	5.61×10^{-16}	-5.570	-4.777
5	^{145}Tm	69	5	1.740	9.44×10^{-16}	-6.195	-5.409
6	^{147}Tm	69	5	1.058	5.39×10^{-22}	0.049	0.591
7	^{150}Lu	71	5	1.270	4.83×10^{-20}	-1.905	-1.180
8	^{151}Lu	71	5	1.241	2.41×10^{-20}	-1.602	-0.896
9	^{155}Ta	73	5	1.776	2.49×10^{-16}	-5.616	-4.921
10	^{156}Ta	73	2	1.014	3.98×10^{-21}	-0.810	-0.620
11	^{157}Ta	73	0	0.935	1.25×10^{-21}	-0.318	-0.523
12	^{160}Re	75	2	1.278	2.25×10^{-18}	-3.572	-3.046
13	^{161}Re	75	0	1.197	1.56×10^{-18}	-3.414	-3.432
14	^{164}Ir	77	5	1.570	1.06×10^{-18}	-3.245	-3.959
15	^{166}Ir	77	2	1.152	3.90×10^{-21}	-1.153	-0.824
16	^{167}Ir	77	0	1.071	8.30×10^{-21}	-1.140	-0.959
17	^{171}Au	79	0	1.452	6.29×10^{-17}	-5.019	-4.770
18	^{177}Tl	81	0	1.162	9.45×10^{-21}	-1.196	-1.174
19	^{185}Bi	83	0	1.543	8.76×10^{-18}	-4.875	-4.229

momentum can be ignored due to the relatively large reduced mass of the cluster-core system [41]. For proton radioactivity, however, the contribution of the angular momentum is very important. The centrifugal barrier has an evident effect on proton radioactivity. In the calculations, therefore, we take into account the contribution of the angular momentum on the half-life of proton radioactivity.

In Table 1, the first three columns list the sequence numbers, parent nuclei and corresponding proton numbers, respectively. The fourth column is the experimental l value [14]. The fifth column denotes the experimental Q values extracted from the latest atomic mass table [44]. The sixth column is the theoretical penetrability factor \mathcal{P} . The seventh and eighth columns list the calculated logarithmic half-lives and the experimental values [14], respectively.

From Table 1, one can see that in most cases the calculated half-lives are in good agreement with the experimental values. All the deviations between the calculated logarithmic half-lives and the experimental data are less than 0.8. The biggest and smallest deviations are 0.793 (in ^{113}Cs) and 0.018 (in ^{161}Re), respectively.

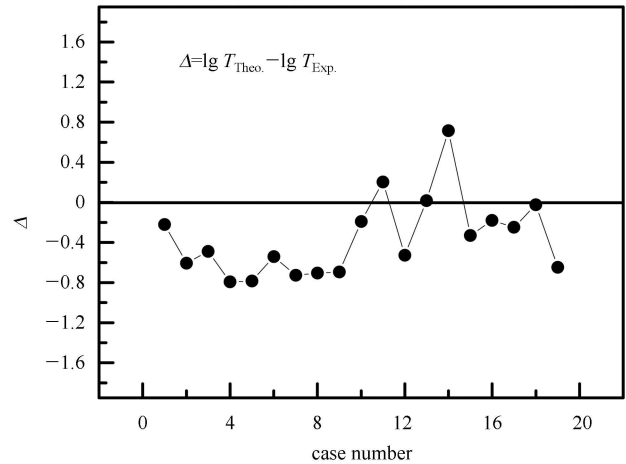
The root-mean-square (rms) deviation between the calculated logarithmic half-lives and the experimental ones is defined as:

$$\sigma = \left[\sum_{i=1}^{19} (\lg T_{\text{Theo.}} - \lg T_{\text{Exp.}})^2 / 19 \right]^{1/2} = 0.523. \quad (11)$$

The rms deviation is small, showing that the present calculations for proton radioactivity are reliable.

For a clear insight into the reliability of the present calculations, we will discuss the theoretical results graphically. The deviations between the calculated logarithmic half-lives and the experimental data are shown in Fig. 2.

One can clearly see from Fig. 2 that the theoretical results are close to the experimental data, with all deviations between the calculated logarithmic half-lives and the experimental data less than 0.8.


 Fig. 2. Deviations between the calculated logarithmic half-lives and experimental data. The deviation is defined as: $\Delta = \lg T_{\text{Theo.}} - \lg T_{\text{Exp.}}$.

The theoretical half-lives show a strong dependence on the orbital angular momentum of the emitted proton. The l values in Table 1 are the values suggested in the experimental literature. It should be pointed out that in all the experiments performed to date, only the half-life

and the energy of the proton are measured. The spin and parity are not experimentally observed quantities — the values given in experimental papers are based on the calculated decay rates. The theoretical results can achieve a better agreement with the experimental data if a suitable l value is employed in the present model.

In [37], ground-state proton radioactivity has been identified from ^{121}Pr . A transition with a half-life $T_{1/2} = 10_{-3}^{+6}$ ms ($\lg T = -2.000$) has been observed and is assigned to the decay of a highly prolate deformed $3/2^+$ or $3/2^-$ Nilsson state. In Fig. 3 we show the variation of the half-life of a proton emission for ^{121}Pr as a function of angular momentum.

The solid line denotes the calculated results. It can be seen that the half-life values have a strong dependence on the orbital angular momentum of the emitted proton. There is an increase of 10 orders of magnitude in the half-life values when the orbital angular momentum varies from 0 to $10\hbar$. The measured half-life (dashed line in Fig. 3) is $\lg T = -2.000$. If the orbital angular momentum is chosen as $l=3$, the calculated value is in excellent agreement with the experimental one.

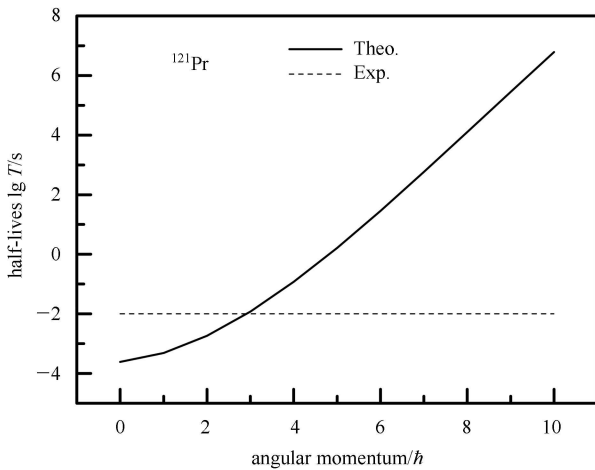


Fig. 3. Angular momentum dependence of the half-life of proton radioactivity for ^{121}Pr .

In [30], proton radioactivity from ^{141}Ho and ^{131}Eu has been identified. The ^{141}Ho proton transition has a half-life $T_{1/2} = 4.2(4)$ ms ($\lg T = -2.376$), and is assigned to the decay of the $7/2^-$ [523] Nilsson state. The ^{131}Eu transition has a half-life $T_{1/2} = 26(6)$ ms ($\lg T = -1.585$), consistent with the decay from either the $3/2^+$ [411] or $5/2^+$ [413] Nilsson orbital. In the present model, the calculated logarithmic half-life is $\lg T = -1.948$ for ^{141}Ho if the orbital angular momentum is chosen as $l = 5$, and the calculated value for ^{131}Eu is $\lg T = -1.186$ if $l = 4$. The calculated results are in good agreement with the experimental ones.

From the above discussions, one can see that the present model is reliable for calculating the half-lives of

proton radioactivity. This gives us confidence to perform theoretical predictions for the possible candidate nuclei for proton radioactivity.

We perform a large number of systematic calculations for half-lives of proton radioactivity throughout the periodic table. From Table 1, the experimental transferred angular momenta are usually $l = 0, 2, 5$. Because the angular momenta carried by the emitted proton of the probable candidate nuclei for proton radioactivity are unknown, the half-lives are calculated under the assumption of the three probable transferred angular momenta ($l=0, 2, 5$).

Table 2. Predicted probable candidate nuclei for proton radioactivity and their calculated half-lives under the three probable transferred angular momenta ($l=0, 2, 5$). The experimental Q values are extracted from [44]. Q value is in MeV, and half-life T is in seconds.

nucleus	Z	Q	$\lg T_{\text{theo.}}$		
			$l=0$	$l=2$	$l=5$
^{42}V	23	0.242	-7.328	-5.824	-1.528
^{50}Co	27	0.098	8.454	9.847	14.449
^{54}Cu	29	0.387	-7.997	-6.678	-2.806
^{55}Cu	29	0.298	-5.325	-4.003	0.024
^{68}Br	35	0.560	-8.571	-7.388	-3.839
^{69}Br	35	0.450	-6.344	-5.160	-1.498
^{73}Rb	37	0.600	-8.373	-7.227	-3.749
^{76}Y	39	0.629	-7.988	-6.874	-3.449
^{81}Nb	41	0.750	-8.960	-7.879	-4.574
^{85}Tc	43	0.852	-9.475	-8.423	-5.206
^{89}Rh	45	0.700	-6.696	-5.670	-2.399
^{104}Sb	51	0.509	0.078	1.028	4.269
^{108}I	53	0.600	-1.394	-0.464	2.691
^{118}La	57	0.378	8.407	9.293	12.445
^{122}Pr	59	0.526	3.448	4.318	7.371
^{126}Pm	61	0.759	-1.492	-0.637	2.305
^{127}Pm	61	0.545	3.795	4.647	7.650
^{130}Eu	63	1.028	-4.974	-4.132	-1.293
^{133}Eu	63	0.675	1.101	1.937	4.860
^{136}Tb	65	0.918	-2.784	-1.960	0.870
^{137}Tb	65	0.759	0.047	0.869	3.735
^{142}Ho	67	0.554	6.340	7.143	10.020
^{148}Tm	69	0.489	9.798	10.585	13.436
^{152}Lu	71	0.833	0.827	1.605	4.350
^{153}Lu	71	0.609	6.384	7.159	9.946
^{162}Re	75	0.764	3.831	4.582	7.272
^{163}Re	75	0.706	5.278	6.027	8.726
^{169}Ir	77	0.621	8.675	9.411	12.088
^{169}Au	79	1.961	-8.808	-8.069	-5.588
^{170}Au	79	1.474	-5.221	-4.485	-1.949
^{172}Au	79	0.900	2.411	3.140	5.747
^{173}Au	79	0.992	0.730	1.459	4.053
^{176}Tl	81	1.250	-2.320	-1.598	0.937
^{178}Tl	81	0.738	6.866	7.581	10.178
^{179}Tl	81	0.727	7.147	7.861	10.458
^{184}Bi	83	1.327	-2.675	-1.964	0.533
^{186}Bi	83	1.083	0.546	1.253	3.775
^{187}Bi	83	1.019	1.579	2.285	4.813

From the calculated results, we only select candidate nuclei with $-10 < \lg T_{\text{Theo.}} < 10$ to display. The predicted probable candidate nuclei and their half-lives for proton radioactivity are listed in Table 2.

At present, theoretical and experimental studies on proton radioactivity are mainly focused on the region $51 \leq Z \leq 83$. In Table 2, we are surprised to find that there are 11 candidate nuclei for proton radioactivity in the $Z < 51$ region, which is a very interesting result. In the region $Z > 83$, we do not find any candidate nuclei for proton radioactivity within our selected range of half-lives ($-10 < \lg T_{\text{Theo.}} < 10$).

4 Summary

In this work, proton radioactivity has been investigated using the effective liquid drop model with varying mass asymmetry shapes and effective inertial coefficients.

In view of the importance of r_0 for this model, a new effective nuclear radius constant formula replaces the old empirical one. The theoretical half-lives are in good agreement with the available experimental data. All the deviations between the calculated logarithmic half-lives and the experimental data are less than 0.8. The rms deviation between the calculated logarithmic half-lives and the experimental ones is 0.523. For proton radioactivity from ^{121}Pr , ^{141}Ho and ^{131}Eu , the calculated half-lives are in good agreement with the experimental values if we select suitable l values in the present model. We make some predictions for half-lives of proton radioactivity throughout the periodic table. We find that there are 11 candidate nuclei for proton radioactivity in the region $Z < 51$. In the region $Z > 83$, we do not find any candidate nuclei for proton radioactivity within our selected half-life range. Our calculated results may be useful for future experiments.

References

- 1 REN Z Z, XU G O. Phys. Rev. C, 1987, **36**: 456
- 2 XU C, REN Z Z. Phys. Rev. C, 2006, **73**: 041301(R)
- 3 REN Y J, REN Z Z. Phys. Rev. C, 2012, **85**: 044608
- 4 ZHU Z L, NIU Z M, LI D P, LIU Q, GUO J Y. Phys. Rev. C, 2014, **89**: 034307
- 5 JIANG W Z. Phys. Rev. C, 2010, **81**: 044306
- 6 JIANG W Z, ZHAO Y L, ZHU Z Y, SHEN S F. Phys. Rev. C, 2005, **72**: 024313
- 7 CAO D L, REN Z Z, DONG T K. Chin. Phys. C, 2013, **37**: 034103
- 8 ZHOU F, GUO J Y. HEP & NP, 2007, **31**: 1106 (in Chinese)
- 9 WANG S H, GUO J Y. HEP & NP, 2006, **30(S2)**: 87 (in Chinese)
- 10 GAN Z G, FAN H M, QIN Z. HEP & NP, 2004, **28**: 332 (in Chinese)
- 11 Jackson K P, Cardinal C U, Evans H C, Jelley N A, Cerny J. Phys. Lett. B, 1970, **33**: 281
- 12 Cerny J, Esterl J E, Gough R A, Sextro R G. Phys. Lett. B, 1970, **33**: 284
- 13 Woods P J, Davis C N. Annu. Rev. Nucl. Part. Sci., 1997, **47**: 541
- 14 Sonzogni A A. Nucl. Data Sheets, 2002, **95**: 1
- 15 Karny M, Rykaczewski K P, Grzywacz R K et al. Phys. Lett. B, 2008, **664**: 52
- 16 Davids Cary N. Nucl. Phys. A, 1998, **630**: 321c
- 17 Arumugam P, Ferreira L S, Maglione E. Phys. Rev. C, 2008, **78**: 041305(R)
- 18 Ferreira L S, Maglione E. Nucl. Phys. A, 2005, **752**: 223c
- 19 Delion D S, Liotta R J, Wyss R. Phys. Rep., 2006, **424**: 113
- 20 Bhattacharya M, Gangopadhyay G. Phys. Lett. B, 2007, **651**: 263
- 21 DONG J M, ZHANG H F, Royer G. Phys. Rev. C, 2009, **79**: 054330
- 22 ZHANG H F, WANG Y J, DONG J M, LI J Q, Scheid W. J. Phys. G: Nucl. Part. Phys., 2010, **37**: 085107
- 23 Aggarwal M. Phys. Lett. B, 2010, **693**: 489
- 24 Routray T R, Tripathy S K, Dash B B, Behera B, Basu D N. Eur. Phys. J. A, 2011, **47**: 92
- 25 Ferreira L S, Maglione E, Ring P. Phys. Lett. B, 2011, **701**: 508
- 26 Routray T R, Mishra A, Tripathy S K, Behera B, Basu D N. Eur. Phys. J. A, 2012, **48**: 77
- 27 DONG J M, ZHANG H F, ZUO W, LI J Q. Chin. Phys. C, 2010, **34**: 182
- 28 WANG J M, ZHANG H F, LI J Q. J. Phys. G: Nucl. Part. Phys., 2014, **41**: 065102
- 29 Davids C N, Woods P J, Batchelder J C et al. Phys. Rev. C, 1997, **55**: 2255
- 30 Davids C N, Woods P J, Seweryniak D et al. Phys. Rev. Lett., 1998, **80**: 1849
- 31 Poli G L, Davids C N, Woods P J et al. Phys. Rev. C, 1999, **59**: R2979
- 32 Poli G L, Davids C N, Woods P J et al. Phys. Rev. C, 2001, **63**: 044304
- 33 Mahmud H, Davids C N, Woods P J et al. Phys. Rev. C, 2001, **64**: 031303(R)
- 34 Rykaczewski K, McConnell J W, Bingham C R et al. Nucl. Phys. A, 2002, **701**: 179c
- 35 Woods P J, Munro P, Seweryniak D et al. Phys. Rev. C, 2004, **69**: 051302(R)
- 36 Mukha I, Roeckl E, Döring J et al. Phys. Rev. Lett., 2005, **95**: 022501
- 37 Robinson A P, Woods P J, Seweryniak D et al. Phys. Rev. Lett., 2005, **95**: 032502
- 38 Page R D, Bianco L, Darby I G et al. Phys. Rev. C, 2007, **75**: 061302(R)
- 39 Procter M G, Cullen D M, Taylor M J et al. Phys. Lett. B, 2013, **725**: 79
- 40 Gonçalves M, Duarte S B. Phys. Rev. C, 1993, **48**: 2409
- 41 Duarte S B, Gonçalves M G. Phys. Rev. C, 1996, **53**: 2309
- 42 SHENG Z Q, NI D D, REN Z Z. J. Phys. G: Nucl. Part. Phys., 2011, **38**: 055103
- 43 Gamow G. Z. Phys. A, 1928, **51**: 204
- 44 WANG M, Audi G, Wapstra A H, Kondev F G, MacCormick M, XU X, Pfeiffe B. Chin. Phys. C, 2012, **36**: 1603
- 45 Duarte S B, Tavares O A P, Guzmán F, Dimarco A. At. Data Nucl. Data Tables, 2002, **80**: 235